soil systems

MDPI

*Article*

# A Novel Approach for High-Frequency *in-situ* Quantification of Methane Oxidation in Peatlands

**Cecilie Skov Nielsen [1,*], Niles J. Hasselquist [1], Mats B. Nilsson [1], Mats Öquist [1], Järvi Järveoja [1] and Matthias Peichl [1]**

[1] Department of Forest Ecology and Management, Swedish University of Agricultural Sciences, Skogsmarksgränd, 90183 Umeå, Sweden; niles.hasselquist@slu.se (N.J.H.); mats.b.nilsson@slu.se (M.B.N.); mats.oquist@slu.se (M.Ö.); jarvi.jarveoja@slu.se (J.J.); matthias.peichl@slu.se (M.P.)

* Correspondence: cecilie.skov.nielsen@slu.se; Tel.: +46-907−868172

Received: 5 October 2018; Accepted: 14 December 2018; Published: 31 December 2018

**Abstract:** Methane ($CH_4$) oxidation is an important process for regulating $CH_4$ emissions from peatlands as it oxidizes $CH_4$ to carbon dioxide ($CO_2$). Our current knowledge about its temporal dynamics and contribution to ecosystem $CO_2$ fluxes is, however, limited due to methodological constraints. Here, we present the first results from a novel method for quantifying *in-situ* $CH_4$ oxidation at high temporal resolution. Using an automated chamber system, we measured the isotopic signature of heterotrophic respiration ($CO_2$ emissions from vegetation-free plots) at a boreal mire in northern Sweden. Based on these data we calculated $CH_4$ oxidation rates using a two-source isotope mixing model. During the measurement campaign, 74 % of potential $CH_4$ fluxes from vegetation-free plots were oxidized to $CO_2$, and $CH_4$ oxidation contributed 20 ± 2.5 % to heterotrophic respiration corresponding to 10 ± 0.5 % of ecosystem respiration. Furthermore, the contribution of $CH_4$ oxidation to heterotrophic respiration showed a distinct diurnal cycle being negligible during nighttime while contributing up to 35 ± 3.0 % during the daytime. Our results show that $CH_4$ oxidation may represent an important component of the peatland ecosystem respiration and highlight the value of our method for measuring *in-situ* $CH_4$ oxidation to better understand carbon dynamics in peatlands.

**Keywords:** Methane oxidation; peatland; heterotrophic respiration; carbon; $CO_2$; mire

## 1. Introduction

Northern peatlands are an important component of the global carbon (C) cycle, as they are sinks of carbon dioxide ($CO_2$) and store about one third of the global soil organic C stock [1]. However, northern peatlands also emit the potent greenhouse gas methane ($CH_4$) at a rate that depends on the balance between $CH_4$ production and oxidation of $CH_4$ to $CO_2$. Detailed knowledge of *in-situ* $CH_4$ production and oxidation dynamics is thus key for understanding the contribution of $CH_4$ from northern peatlands to the atmosphere. Furthermore, as these processes are sensitive to climatic factors [2–4], this understanding is even more crucial in order to accurately predict the role of northern peatlands for the atmospheric radiative forcing under a changing climate.

No studies to our knowledge have measured *in-situ* $CH_4$ oxidation continuously with high temporal resolution in predominantly methanogenic systems, e.g. peatlands, in the field. Furthermore, current studies do not estimate the contribution of $CO_2$ resulting from $CH_4$ oxidation to total ecosystem respiration (ER, abbreviations are listed in Table 1), and thus our understanding of the importance of this process in relation to the other $CO_2$ component fluxes is limited. Most peatland $CO_2$ models assume that all heterotrophic respiration ($R_h$) comes from soil organic matter (SOM) mineralization [5-8] while ignoring the contributions from $CH_4$ oxidation. Meanwhile, those

models that estimate *in-situ* $CH_4$ oxidation lack data for validation [9]. This could potentially result in false parametrization and model predictions and overestimation of SOM mineralization with impacts on the modeling of the C balance. Another important limitation of previous studies is that they do not measure $CH_4$ oxidation continuously and with high temporal resolution, and as a result we know little of the temporal variation of $CH_4$ oxidation on both diurnal and seasonal time scales. This might further affect model prediction and estimation, particularly if input data is measured only during daytime and/or during the peak growing season. These issues therefore highlight the need for high temporal resolution $CH_4$ oxidation data in order to support process-based model development and to further improve our understanding of the peatland C cycle.

**Table 1.** List of abbreviations used in the article

| Term | Abbreviation |
|---|---|
| Concentration of headspace $CH_4$ at time 0 in the incubation experiment for the fractionation factor | $[CH_4]_0$ |
| Concentration of headspace $CH_4$ at time t in the incubation experiment for the fractionation factor | $[CH_4]_t$ |
| Ecosystem respiration | ER |
| Fractional contribution of $CH_4$ oxidation to heterotrophic respiration | $f_{CH4}$ |
| Kinetic fractionation factor | $\alpha$ |
| Heterotrophic respiration | $R_h$ |
| Isotopic $^{13}C$ signature | $\delta^{13}C$ |
| Isotopic $^{13}C$ signature of ecosystem respiration | $\delta^{13}C_{ER}$ |
| Isotopic $^{13}C$ signature of headspace $CH_4$ at times 0 in the incubation experiment for the fractionation factor | $\delta^{13}C_{CH4,0}$ |
| Isotopic $^{13}C$ signature of headspace $CH_4$ at times t in the incubation experiment for the fractionation factor | $\delta^{13}C_{CH4,t}$ |
| Isotopic $^{13}C$ signature of heterotrophic respiration | $\delta^{13}C_{Rh}$ |
| Isotopic $^{13}C$ signature of pore water $CH_4$ | $\delta^{13}C_{CH4,pw}$ |
| Isotopic $^{13}C$ signature of organic matter | $\delta^{13}C_{OM}$ |
| Net ecosystem exchange | NEE |
| Organic matter | OM |
| Permil fractionation factor | $\Delta$ |
| Relative $CH_4$ oxidation % | $\%CH_{4oxi}$ |
| Soil organic matter | SOM |

Current methods for estimating $CH_4$ oxidation in peatlands include laboratory incubations [10-12], often in combination with oxidation inhibitors [13–15], stable isotope techniques [10,16–19], methane profiles [20] and gas push-pull tests [21] which all have their strengths and weaknesses. For instance, the disadvantage of incubations is that they may estimate oxidation potentials instead of actual *in-situ* rates. Meanwhile, oxidation inhibitors are intrusive, do not allow for repeated measurements, and may partly inhibit $CH_4$ production [22,23]. The use of natural abundance stable isotope techniques is promising, although these techniques have traditionally been based on manual sampling which limits the spatial and temporal resolution of these measurements. In addition, natural abundance approaches depend on reliable estimates of the fractionation factors for $CH_4$ oxidation and diffusion [18,24]. Thus, there is a need for new methods that overcome these limitations and allow *in-situ* measurements of $CH_4$ oxidation at high temporal scales to better parameterize C and greenhouse gas dynamics in peatlands.

This study aims at developing a method for continuous high-frequency estimates of peatland $CH_4$ oxidation and the proportion of $R_h$ that emanates from $CH_4$ oxidation. In spring 2014, we established an experimental setup in the field with automated flux chambers connected to a Picarro G1101-*i* isotopic $CO_2$ analyzer (Picarro Inc., Santa Clara, CA, USA) in an oligotrophic, minerogenic mire in northern Sweden. We measured massfluxes and isofluxes of ER and $R_h$ (from plots with all photosynthetic biomass removed). By combining the isotopic signature ($\delta^{13}C$) of $R_h$, organic matter (OM) and pore water $CH_4$ in a two-source mixing model, we were for the first time able to partition the $CO_2$ originating from heterotrophic respiration into $CO_2$ resulting from $CH_4$ oxidation and mineralization of OM.

## 2. Materials and Methods

### *2.1. Site Description*

The field site is an oligotrophic, minerogenic mire, Degerö Stormyr (64°11′ N, 19°33′ E), located near the town of Vindeln, Västerbotten County, Northern Sweden. The average annual temperature and average annual precipitation of the World Meteorological Organization (WMO) reference normal period 1961-1990 is 1.2 °C and 523 mm respectively (Table 2) [25]. Long-term net ecosystem exchange (NEE) is -58 g C $m^{-2}$ $year^{-1}$ [26], average growing season $CH_4$ emission rates are *ca.* 1 to 5 mg $CH_4$ $m^{-2}$ $h^{-1}$ [27], and the net ecosystem carbon balance is *ca.* −20 to −27 g C $m^{-2}$ $year^{-1}$ [28]. Approximately half of the precipitation comes as snow and snow cover lasts for about six months (November to April). The peat layer is on average 3 to 4 m deep and the growing season water table generally varies between ca. 0 and 25 cm [26,28]. The vegetation consists mainly of *Sphagnum majus* Russ. C. Jens., *Sphagnum balticum* Russ. C. Jens., and *Sphagnum lindbergii* Schimp. Ex Lindb, *Eriophorum vaginatum* L., *Trichophorum cespitosum* L. Hartm., *Vaccinium oxycoccos* L., *Andromeda polifolia* L., *Rubus chamaemorus* L[29].

**Table 2.** Climate and soil properties at Degerö Stormyr.

| Properties | Value |
|---|---|
| Mean annual temperature | 1.2 °C [25] |
| Mean annual precipitation | 523 mm [25] |
| Growing season mean water table level | −4.1 cm [30] |
| Average depth of peat layer | 3–4 m [28] |
| Peat C:N ratio [1] | 68.9 ± 1.9 |

[1] 0–30 cm depth.

### *2.2. Experimental Setup*

The experimental setup was established in spring 2014 and consists of four replicate blocks containing three plots (1 × 1 m) each with different treatments, resulting in a total of 12 plots. Thus, each treatment/measurement type has four replicates. Each plot is equipped with an automated chamber (45 × 45 cm, 15 cm high) for flux measurements. A detailed description of the automated chamber system is provided by Järveoja et al. 2018 [30]. Briefly, two plots in each block are undisturbed where one is used for measurements of NEE using a transparent chamber and the other for measurements of ER using a dark chamber. In the third plot within each block, the aboveground vegetation, including the green parts (i.e., ~upper 5 cm) of the *Sphagnum* mosses, was removed in autumn 2013, and a 30 cm deep trench was cut along the plot sides using a handheld saw to prevent root activity inside the plots. These plots were used for measurements of $CO_2$ from heterotrophic activity ($R_h$) with a dark chamber. $CH_4$ fluxes were also measured at all plots. Each automatic flux

chamber has measurements of air temperature 10 cm above the peat surface, and soil temperature at 2 and 10 cm depth. A water level sensor is also placed in each block.

### *2.3. Measurements of Mass and Isotopes of $CH_4$ and $CO_2$*

Fluxes of $CO_2$ and $CH_4$ mass as well as the $\delta^{13}C$ signature of the $CO_2$ concentrations were measured in the period of 18 to 27 July, 2014. Massfluxes of $CO_2$ (NEE, ER, $R_h$) and $CH_4$ were measured using a greenhouse gas analyzer (model GGA-24EP, Los Gatos Research (LGR) Inc., San Jose, CA, USA) connected in a closed loop to the chambers. Isofluxes and massfluxes, used for Keeling plots, were measured using a Picarro G1101-*i* (Picarro Inc., CA, USA) placed downstream of the LGR. Analytical precision *for in-situ* carbon isotope analyses using the Picarro 1101-*i* instrument was 0.2 ‰ based on repeated analysis of known isotopic standards. An external pump was connected to the loop to provide continuous airflow. Chamber closure time lasted 18 min and was preceded and followed by one-minute flushing of the tubes with ambient air before onset of next measurement. Measurements took one hour per block and thus four hours for one round of measurements. The mean time of each four-hour measurement round is used to designate the measurement time point for a four-hour mean flux. For example, the measurement round taking place from 00.00 to 04:00 a.m. is reported for the time point 02:00 a.m.

### *2.4. Isotopic Signature of Soil Organic Matter and Pore Water $CH_4$*

In order to obtain the $\delta^{13}C$ signature of soil organic matter ($\delta^{13}C_{OM}$), eight peat cores from 0 to 30 cm depth, which represents the area of highest potential $CH_4$ production and oxidation activity [31], were collected from the mire in October 2015. The cores were cut into 2 cm sections and freeze-dried. The 2 cm sections were then ground in a ball mill and analyzed for $\delta^{13}C$ signature on an elemental analyzer (Flash EA 2000, Thermo Scientific, Bremen, Germany) coupled to a continuous flow isotope ratio mass spectrometer (IRMS, Delta V Advantage, Thermo Scientific, Bremen, Germany). The standard deviation based on analysis of standards was <0.15‰ for $\delta^{13}C$.

On 3 and 27 August 2015, pore water was collected at 20 and 30 cm just outside the chamber frames in the non-vegetated plots and the vegetated plots used for dark measurements, as well as one location in the middle of the four blocks (n = 30). 2 mL of pore water was sampled using a syringe and transferred to $N_2$ flushed vials. Subsequently, 2 mL of gas was removed from the vials in order to equalize the pressure. The samples were stored at 5 °C until analysis for $\delta^{13}C$ signature of $CH_4$ ($\delta^{13}C_{CH4,pw}$) on a Precon (Thermo Scientific, Bremen, Germany) and a gasbench (GasBench II, Thermo Scientific, Bremen, Germany) connected to a continuous flow IRMS (Delta V Advantage, Thermo Scientific, Bremen, Germany) on 28 and 29 September 2015. The standard deviation based on analysis of standards was <0.3‰ for $\delta^{13}C$.

### *2.5. Incubation Experiment to Determine the Fractionation Factor for $CH_4$ Oxidation*

Four cores of 10 × 10 cm and 20 cm deep were collected in the Degerö mire on 8 October 2017. The cores were divided into four depths 0–5, 5–10, 10–15 and 15–20 cm below live vegetation, put in zip lock bags, brought back to the lab and placed in a freezer (−18 °C). Samples were kept frozen for two months and then preincubated at 4 °C for a month. After preincubation, 10 g field moist peat material from each sub core was transferred to 160 mL airtight glass bottles. Three replicates were made of each sample (to be incubated at three different temperatures) giving a total of 48 bottles (i.e., one sample per layer per core for each temperature). In addition, nine blanks (bottles containing 10 mL water as an analogue for field moist peat) were prepared. All bottles had ambient air inside and were given 0.05 mL pure $CH_4$ to feed the methanotrophs, and placed at 5 °C.

Six days after addition of $CH_4$, two replicate batches of bottles were placed at 10 and 15 °C respectively, while one replicate batch remained at 5 °C. After an additional three days, the bottles were flushed with technical air and given 0.12 mL pure $CH_4$, thereby raising headspace to app. 1000 ppm. Immediately after injecting $CH_4$, 0.5 mL of the headspace was sampled and transferred to 12

mL vials containing helium. Further headspace samples were taken at six, 12, 24, and 48 h and additionally at 96 h for the 0–5 cm interval in order to trace the oxidation rate (i.e., the decrease in headspace $CH_4$ concentration over time, and the concurrent change in $\delta^{13}C$ signature of the $CH_4$). For $^{13}C$ isotope analysis of $CH_4$ in the gas samples, a Finnigan MAT PreCon unit (Thermo Scientific, Bremen, Germany) was used for automated sample conversion and concentration. Briefly, sample $CO_2$ was removed by chemical adsorption succeeded by Pt-catalyzed oxidation of the $CH_4$-component to $CO_2$ that was subsequently trapped by duplicated cryogenic (liquid $N_2$) focusing. The isotopic analysis took place upon separation on a GC (HP 6890, equipped with 25 m long PoraPlot Q fused-silica column (32 mm i.d.), operated at 40 °C) coupled in continuous flow-mode to a Finnigan MAT Delta PLUS isotope ratio mass spectrometer. At the 24-h sampling, an additional 0.5 mL of the headspace was taken out and transferred to a 22 mL vial, where the concentration of $CH_4$ was determined on a gas chromatograph in order to preliminarily assess the oxidation rate and hence the required incubation time (data not shown). By the end of the experiment, the peat samples were dried for 48 h at 60 degrees and weighed for determination of dry weight.

### *2.6. Flux Calculation and Estimation of Flux Isotopic Signature*

Massfluxes of NEE, ER, $R_h$ and $CH_4$ were calculated from the linear change in gas concentration within the chamber headspace over time using the ideal gas law [30]. The linear slope was determined based on 10 concentration records over a 1 min 40 s calculation window (each record representing a 10 s mean of the 1 Hz sampling) moving stepwise (with one-point increments) over the chamber closure period. From these individual slopes, the one with the highest coefficient of determination ($R^2$) was selected as the final slope for each flux measurement. All fluxes with an $R^2 \geq 0.90$ ($p < 0.001$) were accepted giving a total of 428 $CO_2$ flux measurements and 437 $CH_4$ flux measurements over the ten-day period.

The $\delta^{13}C$ source signature of respired $CO_2$ (corresponding to the $\delta^{13}C$ signature of the source material) was determined using the Keeling plot approach [32]. The Picarro G1101-*i* logged measurements approximately every four seconds. From these data, one-minute averages were generated. Disregarding the first one minute average, we used linear regression analysis of $\delta^{13}C$ and $1/[CO_2]$ for the remaining 17 min, with the y-axis intercept corresponding to the $^{13}C$ signature of respired soil $CO_2$. Intercepts were excluded for regressions with slopes not significantly different from 0 ($p > 0.05$) and if the slopes were between −0.25 ppm $min^{-1}$ and 0.25 ppm $min^{-1}$ due to the uncertainty in Keeling estimates associated with very small fluxes.

### *2.7. Calculation of Fractionation Factor for $CH_4$ Oxidation*

To account for preferential use of $^{12}C$ over $^{13}C$ by methanotrophs [33,34], we used a kinetic fractionation factor for $CH_4$ oxidation (hereafter referred to as "fractionation factor" or $\alpha$). The fractionation factor describes the fractionation against the heavy isotope, where $\alpha = 1$ means no fractionation and $\alpha > 1$ means that fractionation is occurring with product becoming depleted in the heavy isotope and the substrate becoming enriched. $\alpha$ was calculated by the following equations [24] based on data from the incubation experiment:

$$\alpha = \frac{1}{(m+1)}, \quad (1)$$

where m is:

$$m = \frac{\delta^{13}C_{CH4,t} - \delta^{13}C_{CH4,0}}{\ln\frac{[CH_4]_t}{[CH_4]_0}}, \quad (2)$$

and $\delta^{13}C_{CH4,0}$ and $\delta^{13}C_{CH4,t}$ designates the $\delta^{13}C$ signature of the headspace $CH_4$ at times 0 and t, and $[CH_4]_0$ and $[CH_4]_t$ is the concentration of the headspace $CH_4$ at times 0 and t. In practice, since we had more than two time points, m was calculated as the slope of a linear regression between the difference in isotopic signatures ($\delta^{13}C_t - \delta^{13}C_0$) and natural logarithm of the fraction between remaining and initial

headspace $CH_4$ concentration ($\ln([CH_4]_t/[CH_4]_0)$) [24]. The permil fractionation factor $\Delta$ could then be calculated from the $\alpha$ [35]:

$$\Delta = \frac{\alpha - 1}{1000}. \quad (3)$$

$CH_4$ oxidation rates were also calculated for the incubations, using linear regression. Only significant fractionation factors (slope different from 0, $p < 0.05$) with a corresponding flux <0 were included in the analysis.

### *2.8. Mixing Model*

The fractional contribution of $CH_4$ oxidation and OM mineralization to total $R_h$ was calculated using a two-source mixing model [35]:

$$f_{CH4} = \frac{\delta_{sample} - \delta^{13}C_{OM}}{\delta^{13}C_{CH4,pw} - \Delta - \delta_{OM}}, \quad (4)$$

where $f_{CH4}$ is the fraction of the heterotrophic respiration contributed by oxidation of $CH_4$, $\delta_{sample}$ is the $\delta^{13}C$ signature of the heterotrophic respiration, $\delta^{13}C_{CH4,pw}$ is the isotopic signature of dissolved $CH_4$ in pore water, and $\delta^{13}C_{OM}$ is the isotopic signature of the OM. We used the mean $\delta^{13}C$ signature of OM in 0–30 cm depth and the mean $\delta^{13}C$ signature of $CH_4$ in 20 and 30 cm depth for the mixing model. We used the mean fractionation factor for methane oxidation in peat at 0–20 cm depth ($\Delta$ = 54.0‰) and across three incubation temperatures (5, 10 and 15 °C) as the statistical test showed no significant effect of neither depth nor temperature. The fractionation factors are subtracted from the $\delta^{13}C_{CH4,pw}$ because the oxidation of $CH_4$ discriminates against the heavy isotope ($^{13}C$) and thus the resulting $CO_2$ is depleted in $^{13}C$ compared to the source $CH_4$. In other words, the $\delta^{13}C$ signature of the $CO_2$ produced during $CH_4$ oxidation is more negative than the source $CH_4$.

The relative contribution of $CH_4$ oxidation ($\%CH_{4oxi}$) is calculated as [36]:

$$\%CH_{4oxi} = \frac{\text{Oxidized } CH_4 \text{ flux}}{\text{Oxidized } CH_4 \text{flux} + \text{measured } CH_4 \text{flux}} * 100, \quad (5)$$

and the oxidized $CO_2$ flux is calculated by multiplying $f_{CH4}$ and $R_h$.

### *2.9. Data Presentation and Statistics*

The differences in fractionation factor between the four depths, and three temperatures were tested with a mixed linear model in R version 3.5.1 (R Core Team, Vienna, Austria) using depth and temperature as fixed effects and core as random effect. The model was reduced stepwise using ANOVA.

All data are presented as mean and standard error. Means and errors for the time series of relative contribution of $CH_4$ oxidation to $R_h$ as well as time series of isotopic signatures of ER and $R_h$ are weighted averages based on the four-hour averages, as some missing values during nighttime would skew an overall average towards daytime values. Figures were made in Sigmaplot 13.0 (Systat Software Inc., San Jose, CA, USA) and R.

## 3. Results and Discussion

### *3.1. Isotopic Signatures of $CO_2$ Fluxes*

Measurements of mass- and isofluxes of ER and $R_h$ as well as fluxes of NEE and $CH_4$ from the undisturbed plots in the mire were carried out from 18 to 27 July 2014 (Figure 1 and Figure S1). During this period, the water table level dropped from 0.08 to 0.16 m below mire surface, and the average daily air temperature at 10 cm above mire surface varied between 8.2 and 30.9 °C (Figure S2). The $\delta^{13}C$ signature of source $CO_2$ in both the ER and $R_h$ fluxes showed strong diurnal cycles (Figure 1). The $\delta^{13}C$ signature of ER ($\delta^{13}C_{ER}$) varied between −52 and −22‰ with minimum values occurring during mid-day. The average of $\delta^{13}C_{ER}$ for the period was −32.3 ± 1.0‰ (±standard error). The four-

hour means of $\delta^{13}C$ signature of $R_h$ ($\delta^{13}C_{Rh}$) usually peaked at 2 am (Figure 1b) with a maximum $\delta^{13}C_{Rh}$ of −22 ‰, whereas the minimum $\delta^{13}C_{Rh}$ was −99‰. Average $\delta^{13}C_{Rh}$ was −49.2 ± 2.3‰.

The observed diurnal pattern of $\delta^{13}C_{ER}$ indicates that given the less depleted source during night, ER mainly results from OM mineralization, whereas during the day, the more depleted signatures of $CO_2$ suggest an additional process contributing to ER. This trend is even more apparent in the vegetation-free $R_h$ plots. We suggest that the source of these negative $\delta^{13}C$ values is the result of methanotrophs oxidizing $CH_4$ with an average $\delta^{13}C$ of −67.2‰ (see below) in the peat pore water. The fact that some $\delta^{13}C_{Rh}$ values were lower than the average $\delta^{13}C$ signature of the $CH_4$ may be due to the uncertainty associated with the estimation of the keeling intercepts (the standard error of the intercept is on average 8.3‰ for $R_h$) or a small difference in $\delta^{13}C_{CH4,pw}$ between the 2014 measurement period and the pore water sampling done in 2015. However, it is also likely due to a large contribution from $CH_4$ oxidation and the fractionation occurring during the oxidation process, which lowers the $\delta^{13}C$ signatures of the resulting $CO_2$ relative to the substrate $CH_4$ [33].

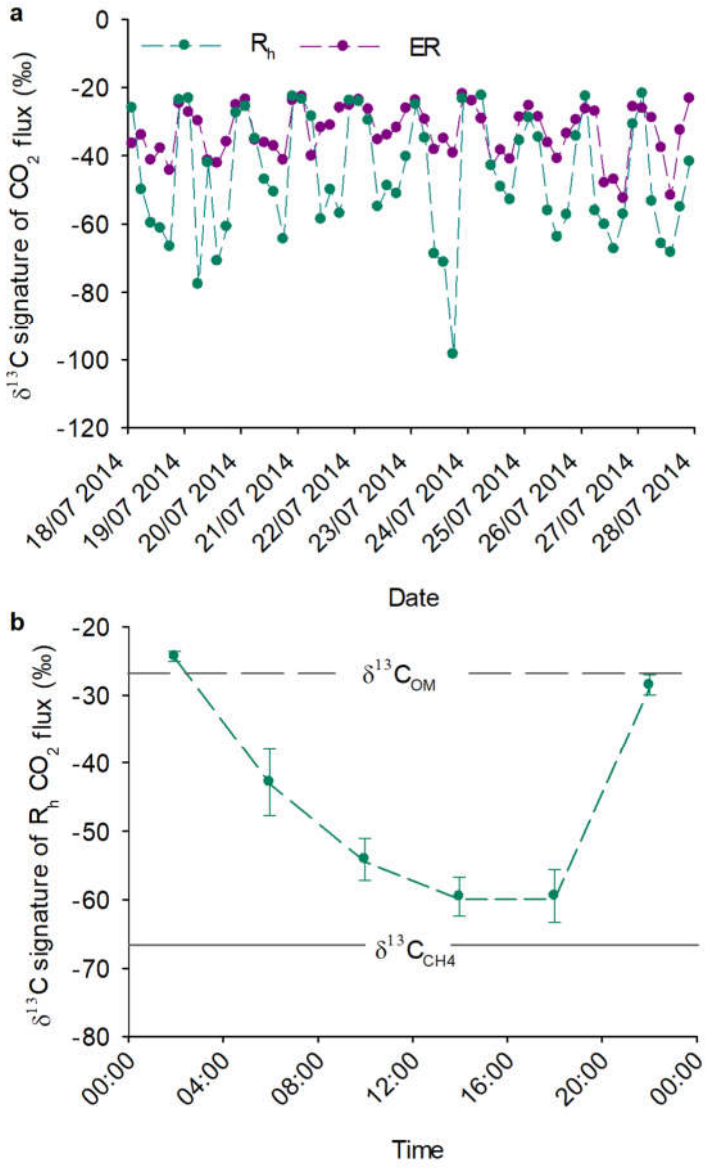


**Figure 1 a)** Four-hourly averages of the carbon isotopic signatures of ecosystem respiration (ER) and heterotrophic respiration ($R_h$) and **b)** average diurnal variation during 18 to 27 July, 2014 in the

isotopic signature of $CO_2$ fluxes from the $R_h$ plots (i.e. plots that had all photosynthetic biomass removed). Error bars in b) show standard error. Dashed and solid lines in b) show respectively the $\delta^{13}C$ signatures of organic matter ($\delta^{13}C_{OM}$) and pore water $CH_4$ ($\delta^{13}C_{CH4,pw}$) in the peatland. The lines connecting the points are visual aids.

### *3.2. Mixing Model*

We used a two-source mixing model to quantify the relative contributions of OM mineralization and $CH_4$ oxidation to total $R_h$ fluxes. The $\delta^{13}C$ signature of OM ($\delta^{13}C_{OM}$) integrated over 0 to 30 cm depth was −27.4‰ (Figure S3) and was used to represent the $\delta^{13}C$ signature of OM mineralization in the mixing model. The average $\delta^{13}C$ signature of the pore water $CH_4$ ($\delta^{13}C_{CH4,pw}$) was −67.2‰ and represents the $\delta^{13}C$ signature of $CO_2$ originating from $CH_4$ oxidation in the mixing model. We consider the $\delta^{13}C_{CH4,pw}$ in 2015 a good representation of the $\delta^{13}C_{CH4,pw}$ from 2014 due to little variation between years in these depths below the water table (−73.4 ± 0.5‰ on 8 August 2017 and −68.1 ± 0.6‰ on 26 July 2018). In order to account for the fractionation taking place when $CH_4$ is oxidized to $CO_2$, we subtracted the measured fractionation factor $\Delta$ = 54.0 ± 3.4‰ (n = 28) from the $\delta^{13}C_{CH4,pw}$ (Figure S4). Our fractionation factor is within the range reported in the literature [19,24,33,37–39] though slightly on the high end. Over the measurement period ( 18 to 27 July 2014) $CH_4$ oxidation contributed 20 ± 2.5% of $R_h$ (Figure 2a) and 10 ± 0.5 % of ER (Figure S1, assuming that no additional oxidation occurs in vegetated plots due to production and transport of oxygen by plants). At the same time, if ignoring any difference in transport rate between $CH_4$ and $CO_2$, 74 % of the produced $CH_4$ in the $R_h$ plots were oxidized to $CO_2$ within the assessed time period. We made a sensitivity analysis to assess the effect of the calculated contribution of $CH_4$ oxidation to $R_h$ using the minimum and maximum measured $\delta^{13}C_{OM}$ and $\delta^{13}C_{CH4,pw}$ as well as minimum and maximum fractionation factors from the literature (Figures S7 and S8). The analysis showed that the highest and lowest estimates across this period resulted in methane oxidation contributing between 16 and 57 % of $R_h$. Our result (20 %) is therefore in the lower range, making it more likely that we underestimate the relative contribution of methane oxidation to soil $CO_2$ effluxes. Using this novel approach our results showed that during a relatively warm and dry period (Figure S2), $CH_4$ oxidation likely reduced $CH_4$ emissions and contributed considerably to $R_h$ in this boreal peatland. Although our approach appears promising in quantifying methane oxidation in real time in the field, our results also stress that more high-frequency measurements are needed to quantify the importance of this process for various mire plant communities and during various stages of the growing season associated with differences in plant phenology, water table levels, and soil temperatures.

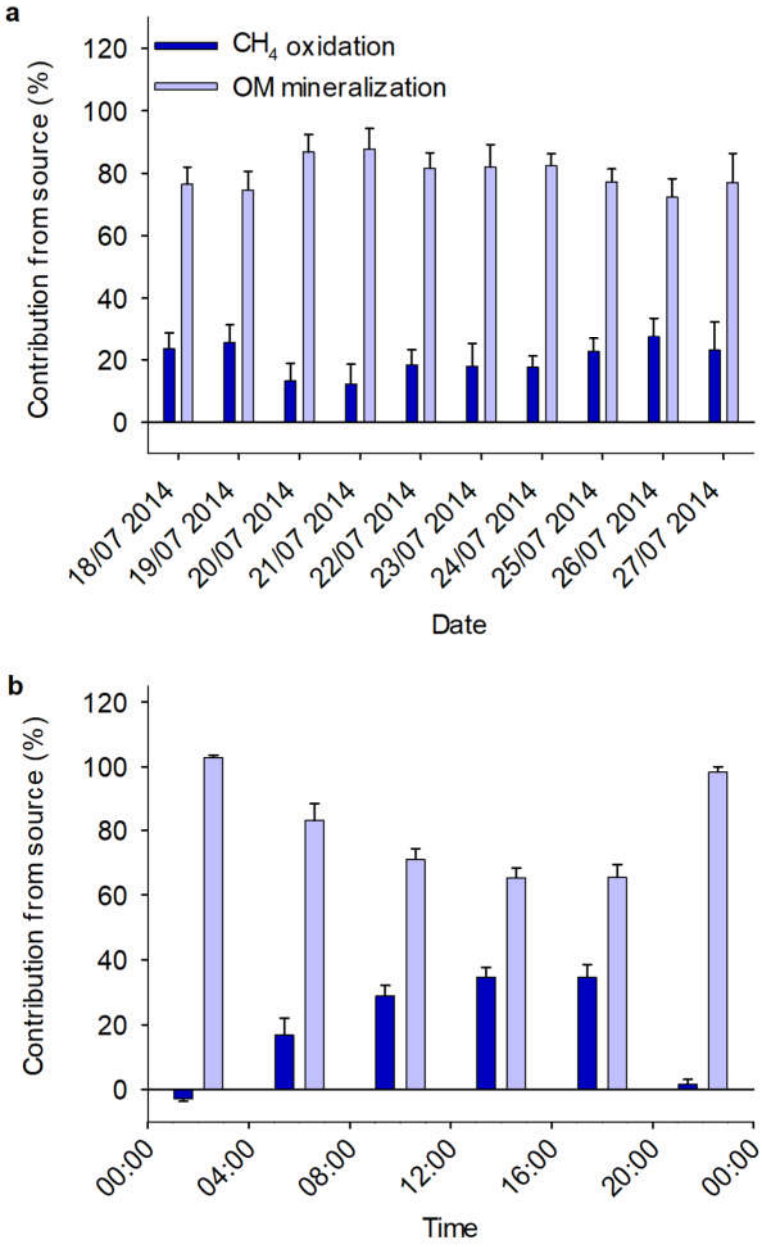


**Figure 2.** The relative contribution of $CH_4$ oxidation and organic matter (OM) mineralization to heterotrophic respiration for the period 18 to 27 July 2014 shown as (**a**) daily averages and (**b**) diurnal ensembles. Error bars show standard error. The negative contribution from $CH_4$ oxidation to $R_h$ at 2 AM is an artifact of uncertainty in the estimation.

### *3.3. Diurnal Variation*

We also observed a diurnal variation in the relative contribution of $CH_4$ oxidation to total $CO_2$ efflux from the $R_h$ plots (Figure 2b). Previously, speculations around diurnal variation in peatland $CH_4$ oxidation have been inferred based on diurnal variation of $CH_4$ fluxes [40]. However, this study shows diurnal variation the isotopic signature of $R_h$ and thus likely in $CH_4$ oxidation. During nighttime, the contribution of $CH_4$ oxidation to $R_h$ seemed negligible, while during the day, $CH_4$ oxidation appeared to contribute up to 35 ± 3.0%. In order to assess whether the diurnal variation was caused by a change in $CH_4$ oxidation rather than increased OM mineralization during night, we

calculated the $CO_2$ fluxes associated with the two processes (Figure S5). These fluxes show that even though mineralization like total $R_h$ appears to be higher during night, there still seems to be a distinct diurnal pattern in the $CH_4$ oxidation. We suggest that the diurnal variation is driven by a combination of changes in soil temperature (on average 7.1 and 2.6 °C difference between min. and max. temperatures in 2 and 10 cm depth respectively, Figure S2) and a decreasing water table. The water table follows a staircase-like trend with lowering during day and plateauing at night (Figure S2) and is likely driven by enhanced evapotranspiration during the day. This would lead to daytime $O_2$ intrusion into areas in the soil profile with high $CH_4$ concentration (enhancing $CH_4$ oxidation rates), as well as to the possible release of $CO_2$ with a depleted signature (originating from $CH_4$) due to enhanced diffusion rates [41]. It is important to point out that the diurnal variation in the isotopic signature of $CO_2$ from vegetated plots may also partly be caused by increased input of $O_2$ to the rhizosphere by photosynthesizing plants. Although it was beyond the scope of this study, the observed diurnal variation in methane oxidation highlights the need for depth specific $O_2$ and $CH_4$ measurements in order to better understand the drivers responsible for temporal variation in methane oxidation in the field. The diurnal variation in $\delta^{13}C$ signatures of $R_h$ also highlights that bias in the diurnal sampling protocol can influence the results as e.g. only daytime sampling would give values highly biased towards more depleted $\delta^{13}C$ signatures. It should also be noted, that there was a buildup of $CO_2$ and $CH_4$ in the air above the mire surface during each night of the measurement period, which may have led to some overestimation of the flux isotopic signature [42,43] (see Figure S6).

Our results show that $CH_4$ oxidation may contribute considerably to $R_h$ fluxes, and thus highlights the importance of including this process in peatland $CO_2$ models in order to better predict and understand peatland C dynamics. Our new approach for measuring $CH_4$ oxidation creates the opportunity for future studies to provide the necessary data to validate and improve these models. Furthermore, studies estimating ecosystem respiration in boreal peatlands based on partitioning of eddy covariance data assume that OM mineralization and plant respiration are the only sources for respired $CO_2$ and commonly relate ecosystem respiration to only one factor; namely temperature [44,45]. However, our results show that in peatland ecosystems a considerable amount of $R_h$ fluxes could be derived from $CH_4$ oxidation which is controlled by additional factors (e.g. water table level [46] and $CH_4$ and $O_2$ availability [47]), that differ from the main factors controlling OM mineralization and plant respiration.

### *3.4. Methodological Limitations*

In our two-source mixing model, we assume that fractionation during diffusion of $CH_4$ and $CO_2$ would not strongly influence our results for the following reasons (1) our estimates of the source $\delta^{13}C$ signatures integrate over the soil profile, (2) there was no difference in the $\delta^{13}C_{CH4,pw}$ at depths 20 and 30 cm, and (3) $CH_4$ diffusion in water saturated soil causes negligible fractionation [24] and in addition other non-fractionating transport processes such as pressure gradients and near surface layer air flow might have contributed to the total flux [48]. We also assume that OM mineralization and aerobic $CH_4$ oxidation are the only two processes influencing the isotopic signature of $^{13}CO_2$ from the $R_h$ plots. Although it is possible that anaerobic $CH_4$ oxidation could potentially take place [49,50], we consider this process of minor importance in this nutrient-poor ecosystem. However, if anaerobic $CH_4$ oxidation was occurring, it would produce $CH_4$ less depleted in $^{13}C$ due to a lower fractionation factor [50] and thereby, if anything, our estimates of contribution of $CH_4$ oxidation to total $R_h$ would be underestimated. We also acknowledge that $CO_2$ is produced during methanogenesis. Theoretically, both hydrogenotrophic (based on carbohydrate fermentation and including the step of $H_2$ production) and acetoclastic methanogenesis produces equimolar amounts of $CO_2$ and $CH_4$, and as the $CH_4$ is depleted compared to the substrate, the $CO_2$ must be equally enriched [51]. An estimation by Corbett and colleagues [51] based on a substrate signature of −26‰ and a resulting $CH_4$ signature of −60‰, suggested a $^{13}C$ signature of 8‰ for the $CO_2$ produced during methanogenesis [51]. In the current study, we were not able to include the $CO_2$ from methanogenesis

in our mixing model, and therefore our estimation of the contribution of $CH_4$ oxidation to total $R_h$ is potentially underestimated. This is because the $CO_2$ from methanogenesis raises the isotopic signature of the total pore water $CO_2$ pool and emitted $CO_2$ and thereby causes the contribution from $CH_4$ oxidation to appear smaller.

We used the method of plant removal and plot trenching for estimating $R_h$ [52]. As is the case for other methods measuring $R_h$, this approach has some shortcomings. For instance, the removal of the vegetation causes a reduction in supply of rhizodeposits and possibly a lower input of $O_2$ to the soil (due to elimination of downward plant mediated transport of $O_2$). For $CH_4$ oxidation, the latter is mostly relevant when the water table is high and thus limits the diffusion of $O_2$ from the atmosphere into soil, as was not the case during our measurement campaign. The decrease in concentration of both $O_2$ and rhizodeposits may however be counteracted to some extent by lateral transfer with moving water, and we consider this issue of minor importance in our study. The plant removal in the $R_h$ plot also eliminated $CH_4$ transport by plants, and thus the $CH_4$ fluxes from these plots were on average 16% lower than from the vegetated plots. In addition, the potential for $CH_4$ oxidization in the vegetation-free plots might also be somewhat lower to due to the removal of the upper moss layer with its associated methanotrophic communities [53]. However, the oxidation in these plots was on average 74 % of potential fluxes, which is marginally higher than the 70 % oxidation in vegetated plots, and thus we would argue that vascular plant $CH_4$ transport and moss-associated $CH_4$ oxidation plays only a minor role for net $CH_4$ oxidation in our experiment.

In this study we used an average of the measured fractionation factors across peat depth and incubation temperature as we found no statistical effect of these parameters. We did, however, find a correlation between oxidation rate and fractionation factor (Figure S9), although we were not able to include this information into the mixing model at this point, as we are using the model to estimate the oxidation rate. We acknowledge however that the fractionation factor can vary in response to different parameters such as $CH_4$ concentration and $CH_4$ oxidation rate [54,55]. The fractionation factor may be positively correlated with $CH_4$ starting concentration of in incubations [54] highlighting the importance of matching the $CH_4$ starting concentration of incubations with conditions found in the field. The fractionation factor is also influenced by the fraction of active methanotrophs [55] and thus a decreasing water table could initially influence the fractionation factor when exposing potentially dormant methanotrophs to optimal conditions. However, according to our sensitivity analysis (Figure S8) this factor alone cannot explain the observed diurnal variation in $CH_4$ oxidation. We encourage future studies for improvements on this method by including this component.

## 4. Conclusions

In this study, we present a new method for continuous, high-frequency *in-situ* quantification of $CH_4$ oxidation in peatlands. Previous studies from wetlands and lakes have quantified $CH_4$ oxidation using the $\delta^{13}C$ (and $\delta D$) of pore water or lake water $CH_4$ [19,33,37] and $CH_4$ flux [56]. However, our method is the first, to our knowledge, that uses high temporal resolution isotopic measurements of $^{13}CO_2$ in $R_h$ fluxes based on automated chamber measurements on vegetation-free plots to quantify the relative contribution of $CH_4$ oxidation to the heterotrophic and ecosystem respiration fluxes in the field. Thus, our approach creates an unprecedented opportunity to study the temporal dynamics and controls of $CH_4$ oxidation in peatland ecosystems. In addition, we observed a diurnal pattern in the $\delta^{13}C$ signatures of heterotrophic respiration suggesting a high contribution of $CH_4$ oxidation to $CO_2$ fluxes during daytime and a negligible contribution during nighttime. Overall, our novel approach of directly measuring the isotopic composition of $R_h$ at high temporal resolution provides unique insight into the effect of $CH_4$ oxidation on $CO_2$ and $CH_4$ fluxes, which is crucial for further developing process-based models and improving our understanding of peatland C dynamics.

**Supplementary Materials:** The following are available online at www.mdpi.com/xxx/s1, Figure S1. $CO_2$ and $CH_4$ fluxes, Figure S2. PAR, temperature and water table data, Figure S3. Carbon isotopic signature of peat, Figure S4. Fractionation factors, Figure S5. $CO_2$ fluxes from $CH_4$ oxidation and OM mineralization, Figure S6. Ambient air $CO_2$ concentrations and isotopic signatures, Figure S7. Sensitivity analysis of daily averages, Figure

S8. Sensitivity analysis of hourly averages, Figure S9. Correlation between fractionation factor and oxidation rate, Table S1. Sensitivity analysis of contribution of $CH_4$ oxidation to heterotrophic respiration.

**Author Contributions:** Conceptualization, N.J.H., M.B.N., M.Ö. and M.P.; Formal analysis, C.S.N., N.J.H. and J.J.; Funding acquisition, M.B.N.; Investigation, C.S.N., N.J.H. and M.P.; Methodology, C.S.N., N.J.H., M.B.N., M.Ö. and M.P.; Visualization, C.S.N.; Writing—original draft, C.S.N.; Writing—review & editing, C.S.N., N.J.H., M.B.N., M.Ö., J.J. and M.P.

**Funding:** This research was funded by the Kempe Foundation, grant number JCK-1608 and Carl Tryggers Foundation grant number CTS 15-377.

**Acknowledgments:** We kindly acknowledge support from the ICOS Sweden (Integrated Carbon Observation System) and SITES (Swedish Infrastructure for Ecosystem Research) research infrastructure funded by the Swedish Research Council and partner research institutes.

**Conflicts of Interest:** The authors declare no conflict of interest.

## References

1. Loisel, J.; Yu, Z.C.; Beilman, D.W.; Camill, P.; Alm, J.; Amesbury, M.J.; Anderson, D.; Andersson, S.; Bochicchio, C.; Barber, K.; et al. A database and synthesis of northern peatland soil properties and Holocene carbon and nitrogen accumulation. *Holocene* **2014**, *24*, 1028–1042, doi:10.1177/0959683614538073.
2. Christensen, T.R.; Ekberg, A.; Ström, L.; Mastepanov, M.; Panikov, N.; Öquist, M.; Svensson, B.H.; Nykanen, H.; Martikainen, P.J.; Oskarsson, H. Factors controlling large scale variations in methane emissions from wetlands. *Geophys. Res. Lett.* **2003**, *30*, doi:Artn 141410.1029/2002gl016848.
3. McCalley, C.K.; Woodcroft, B.J.; Hodgkins, S.B.; Wehr, R.A.; Kim, E.H.; Mondav, R.; Crill, P.M.; Chanton, J.P.; Rich, V.I.; Tyson, G.W.; et al. Methane dynamics regulated by microbial community response to permafrost thaw. *Nature* **2014**, *514*, 478–481, doi:10.1038/nature13798.
4. Granberg, G.; Mikkela, C.; Sundh, I.; Svensson, B.H.; Nilsson, M. Sources of spatial variation in methane emission from mires in northern Sweden: A mechanistic approach in statistical modeling. *Glob. Biogeochem. Cycle* **1997**, *11*, 135–150, doi:10.1029/96gb03352.
5. Wu, Y.Q.; Verseghy, D.L.; Melton, J.R. Integrating peatlands into the coupled Canadian Land Surface Scheme (CLASS) v3.6 and the Canadian Terrestrial Ecosystem Model (CTEM) v2.0. *Geosci. Model Dev.* **2016**, *9*, 2639–2663, doi:10.5194/gmd-9-2639-2016.
6. Wu, J.H.; Roulet, N.T.; Nilsson, M.; Lafleur, P.; Humphreys, E. Simulating the Carbon Cycling of Northern Peat lands Using a Land Surface Scheme Coupled to a Wetland Carbon Model (CLASS3W-MWM). *Atmos.-Ocean* **2012**, *50*, 487–506, doi:10.1080/07055900.2012.730980.
7. Abdalla, M.; Hastings, A.; Bell, M.J.; Smith, J.U.; Richards, M.; Nilsson, M.B.; Peichl, M.; Lofvenius, M.O.; Lund, M.; Helfter, C.; et al. Simulation of $CO_2$ and Attribution Analysis at Six European Peatland Sites Using the ECOSSE Model. *Water Air Soil Poll.* **2014**, *225*, 14, doi:10.1007/s11270-014-2182-8.
8. Qiu, C.; Zhu, D.; Ciais, P.; Guenet, B.; Krinner, G.; Peng, S.; Aurela, M.; Bernhofer, C.; Brümmer, C.; Bret-Harte, S.; et al. ORCHIDEE-PEAT (revision 4596), a model for northern peatland $CO_2$, water and energy fluxes on daily to annual scales. *Geosci. Mod. Dev. Discuss.* **2017**, doi:10.5194/gmd-2017-155.
9. Metzger, C.; Nilsson, M.B.; Peichl, M.; Jansson, P.E. Parameter interactions and sensitivity analysis for modelling carbon heat and water fluxes in a natural peatland, using CoupModel v5. *Geosci. Model Dev.* **2016**, *9*, 4313–4338, doi:10.5194/gmd-9-4313-2016.
10. Gerard, G.; Chanton, J. Quantification of methane oxidation in the rhizosphere of emergent aquatic macrophytes: Defining upper limits. *Biogeochemistry* **1993**, *23*, 79–97, doi:10.1007/Bf00000444.
11. Kankaala, P.; Bergström, I. Emission and oxidation of methane in *Equisetum fluviatile* stands growing on organic sediment and sand bottoms. *Biogeochemistry* **2004**, *67*, 21–37, doi:10.1023/B:BIOG.0000015277.17288.7a.
12. Sundh, I.; Mikkela, C.; Nilsson, M.; Svensson, B.H. Potential Aerobic Methane Oxidation in a Sphagnum-Dominated Peatland—Controlling Factors and Relation to Methane Emission. *Soil Biol. Biochem.* **1995**, *27*, 829–837, doi:10.1016/0038-0717(94)00222-M.
13. Ding, W.X.; Cai, Z.C.; Tsuruta, H. Factors affecting seasonal variation of methane concentration in water in a freshwater marsh vegetated with *Carex lasiocarpa*. *Biol. Fert. Soils* **2005**, *41*, 1-8, doi:10.1007/s00374-004-0812-9.

14. Lombardi, J.E.; Epp, M.A.; Chanton, J.P. Investigation of the methyl fluoride technique for determining rhizospheric methane oxidation. *Biogeochemistry* **1997**, *36*, 153–172, doi:10.1023/a:1005750201264.
15. van der Nat, F.; Middelburg, J.J. Seasonal variation in methane oxidation by the rhizosphere of *Phragmites australis* and *Scirpus lacustris*. *Aquat. Bot.* **1998**, *61*, 95–110, doi:10.1016/s0304-3770(98)00072-2.
16. Popp, T.J.; Chanton, J.P.; Whiting, G.J.; Grant, N. Methane stable isotope distribution at a *Carex* dominated fen in north central Alberta. *Glob. Biogeochem. Cycle* **1999**, *13*, 1063–1077, doi:10.1029/1999gb900060.
17. Groot, T.T.; Bodegom, P.M.V.; Harren, F.J.M.; Meijer, H.A.J. Quantification of methane oxidation in the rice rhizosphere using $^{13}C$-labelled methane. *Biogeochemistry* **2003**, *64*, 355–372, doi:10.2307/1469748.
18. Riveros-Iregui, D.A.; King, J.Y. Isotopic Evidence of Methane Oxidation across the Surface Water-Ground Water Interface. *Wetlands* **2008**, *28*, 928–937, doi:10.1672/07-191.1.
19. Cadieux, S.B.; White, J.R.; Sauer, P.E.; Peng, Y.B.; Goldman, A.E.; Pratt, L.M. Large fractionations of C and H isotopes related to methane oxidation in Arctic lakes. *Geochim. Cosmochim. Acta* **2016**, *187*, 141–155, doi:10.1016/j.gca.2016.05.004.
20. Fechner, E.J.; Hemond, H.F. Methane transport and oxidation in the unsaturated zone of a Sphagnum peatland. *Glob. Biogeochem. Cycles* **1992**, *6*, 33–44, doi:10.1029/91GB02989.
21. Urmann, K.; Gonzalez-Gil, G.; Schroth, M.H.; Zeyer, J. Quantification of Microbial Methane Oxidation in an Alpine Peat Bog. *Vadose Zone J.* **2007**, *6*, 705–712, doi:10.2136/vzj2006.0185
22. King, G.M. In situ analyses of methane oxidation associated with the roots and rhizomes of a bur reed, *Sparganium eurycarpum*, in a Maine wetland. *Appl. Environ. Microbiol.* **1996**, *62*, 4548–4555.
23. Popp, T.J.; Chanton, J.P.; Whiting, G.J.; Grant, N. Evaluation of methane oxidation in the rhizosphere of a *Carex* dominated fen in north central Alberta, Canada. *Biogeochemistry* **2000**, *51*, 259-281, doi:10.1023/a:1006452609284.
24. Preuss, I.; Knoblauch, C.; Gebert, J.; Pfeiffer, E.M. Improved quantification of microbial $CH_4$ oxidation efficiency in arctic wetland soils using carbon isotope fractionation. *Biogeosciences* **2013**, *10*, 2539-2552, doi:10.5194/bg-10-2539-2013.
25. Alexandersson, H.; Karlström, C.; Larsson-Mccann, S. *Temperature and Precipitation in Sweden during 1961–1990. Reference Normals*; SMHI Meteorologi: Norrköping, Sweden, 1991; Volume 81.
26. Peichl, M.; Öquist, M.; Löfvenius, M.O.; Ilstedt, U.; Sagerfors, J.; Grelle, A.; Lindroth, A.; Nilsson, M.B. A 12-year record reveals pre-growing season temperature and water table level threshold effects on the net carbon dioxide exchange in a boreal fen. *Environ. Res. Lett.* **2014**, *9*, 11, doi:10.1088/1748-9326/9/5/055006.
27. Eriksson, T.; Öquist, M.G.; Nilsson, M.B. Effects of decadal deposition of nitrogen and sulfur, and increased temperature, on methane emissions from a boreal peatland. *J. Geophys. Res.-Biogeosci.* **2010**, *115*, 13, doi:10.1029/2010jg001285.
28. Nilsson, M.; Sagerfors, J.; Buffam, I.; Laudon, H.; Eriksson, T.; Grelle, A.; Klemedtsson, L.; Weslien, P.; Lindroth, A. Contemporary carbon accumulation in a boreal oligotrophic minerogenic mire—A significant sink after accounting for all C-fluxes. *Glob. Chang. Biol.* **2008**, *14*, 2317–2332, doi:10.1111/j.1365-2486.2008.01654.x.
29. Laine, A.M.; Bubier, J.; Riutta, T.; Nilsson, M.B.; Moore, T.R.; Vasander, H.; Tuittila, E.-S. Abundance and composition of plant biomass as potential controls for mire net ecosytem $CO_2$ exchange. *Botany* **2011**, *90*, 63–74, doi:10.1139/b11-068.
30. Järveoja, J.; Nilsson, M.B.; Gažovič, M.; Crill, P.M.; Peichl, M. Partitioning of the net $CO_2$ exchange using an automated chamber system reveals plant phenology as key control of production and respiration fluxes in a boreal peatland. *Glob. Chang. Biol.* **2018**, *24*, 8, 3436–3451, doi:10.1111/gcb.14292.
31. Eriksson, T.; Öquist, M.G.; Nilsson, M.B. Production and oxidation of methane in a boreal mire after a decade of increased temperature and nitrogen and sulfur deposition. *Glob. Change Biol.* **2010**, *16*, 2130–2144, doi: 10.1111/j.1365-2486.2009.02097.x.
32. Keeling, C.D. The Concentration and Isotopic Abundances of Atmospheric Carbon Dioxide in Rural Areas. *Geochim. Cosmochim. Acta* **1958**, *13*, 322-334, doi: 10.1016/0016-7037(58)90033-4.
33. Happell, J.D.; Chanton, J.P.; Showers, W.S. The Influence of Methane Oxidation on the Stable Isotopic Composition of Methane Emitted from Florida Swamp Forests. *Geochim. Cosmochim. Acta* **1994**, *58*, 4377-4388, doi: 10.1016/0016-7037(94)90341-7.
34. Coleman, D.D.; Risatti, J.B.; Schoell, M. Fractionation of Carbon and Hydrogen Isotopes by Methane-Oxidizing Bacteria. *Geochim. Cosmochim. Acta* **1981**, *45*, 1033-1037, doi: 10.1016/0016-7037(81)90129-0.

35. Fry, B. *Stable Isotope Ecology*; Springer: New York, NY, USA, 2006; p. 316.
36. Schipper, L.A.; Reddy, K.R. Determination of methane oxidation in the rhizosphere of *Sagittaria lancifolia* using methyl fluoride. *Soil Sci. Soc. Am. J.* 1996, *60*, 611-616.
37. Kankaala, P.; Taipale, S.; Nykanen, H.; Jones, R.I. Oxidation, efflux, and isotopic fractionation of methane during autumnal turnover in a polyhumic, boreal lake. *J. Geophys. Res.-Biogeosci.* **2007**, *112*, doi:Artn G0200310.1029/2006jg000336.
38. De Visscher, A.; De Pourcq, I.; Chanton, J. Isotope fractionation effects by diffusion and methane oxidation in landfill cover soils. *J. Geophys. Res.-Atmos.* **2004**, *109*, 8, doi:10.1029/2004jd004857.
39. Reeburgh, W.S.; Hirsch, A.I.; Sansone, F.J.; Popp, B.N.; Rust, T.M. Carbon kinetic isotope effect accompanying microbial oxidation of methane in boreal forest soils. *Geochim. Cosmochim. Acta* **1997**, *61*, 4761-4767, doi: 10.1016/S0016-7037(97)00277-9.
40. Mikkelä, C.; Sundh, I.; Svensson, B.H.; Nilsson, M. Diurnal variation in methane emission in relation to the water table, soil temperature, climate and vegetation cover in a Swedish acid mire. *Biogeochemistry* **1995**, *28*, 93-114, doi:10.1007/bf02180679.
41. Moore, T.R.; Dalva, M. The influence of temperature and water table position on carbon dioxide and methane emissions from laboratory columns of peatland soils. *J. Soil Sci.* **1993**, *44*, 651-664, doi:10.1111/j.1365-2389.1993.tb02330.x.
42. van Asperen, H.; Warneke, T.; Sabbatini, S.; Höpker, M.; Nicolini, G.; Chiti, T.; Papale, D.; Böhm, M.; Notholt, J. Diel variation in isotopic composition of soil respiratory $CO_2$ fluxes: The role of non-steady state conditions. *Agric. For. Meteorol.* **2017**, *234-235*, 95-105, doi: 10.1016/j.agrformet.2016.12.014.
43. Braendholt, A.; Larsen, K.S.; Ibrom, A.; Pilegaard, K. Overestimation of closed-chamber soil $CO_2$ effluxes at low atmospheric turbulence. *Biogeosciences* **2017**, *14*, 1603-1616, doi:10.5194/bg-14-1603-2017.
44. Lasslop, G.; Reichstein, M.; Papale, D.; Richardson, A.D.; Arneth, A.; Barr, A.; Stoy, P.; Wohlfahrt, G. Separation of net ecosystem exchange into assimilation and respiration using a light response curve approach: Critical issues and global evaluation. *Glob. Chang. Biol.* **2010**, *16*, 187–208, doi:10.1111/j.1365-2486.2009.02041.x.
45. Reichstein, M.; Falge, E.; Baldocchi, D.; Papale, D.; Aubinet, M.; Berbigier, P.; Bernhofer, C.; Buchmann, N.; Gilmanov, T.; Granier, A.; et al. On the separation of net ecosystem exchange into assimilation and ecosystem respiration: Review and improved algorithm. *Glob. Chang. Biol.* **2005**, *11*, 1424–1439, doi:10.1111/j.1365-2486.2005.001002.x.
46. Roslev, P.; King, G.M. Regulation of methane oxidation in a freshwater wetland by water table changes and anoxia. *FEMS Microbiol. Ecol.* **1996**, *19*, 105-115, doi:10.1016/0168-6496(95)00084-4.
47. Lai, D.Y.F. Methane Dynamics in Northern Peatlands: A Review. *Pedosphere* **2009**, *19*, 409-421, doi:10.1016/S1002-0160(09)00003-4.
48. Redeker, K.R.; Baird, A.J.; Teh, Y.A. Quantifying wind and pressure effects on trace gas fluxes across the soil–atmosphere interface. Biogeosciences **2015**, *12*, 7423–7434.
49. Smemo, K.A.; Yavitt, J.B. Anaerobic oxidation of methane: An underappreciated aspect of methane cycling in peatland ecosystems? *Biogeosciences* 2011, 8, 779-793, doi:10.5194/bg-8-779-2011.
50. Smemo, K.A.; Yavitt, J.B. Evidence for Anaerobic $CH_4$ Oxidation in Freshwater Peatlands. *Geomicrobiol. J.* **2007**, *24*, 583-597, doi:10.1080/01490450701672083.
51. Corbett, J.E.; Tfaily, M.M.; Burdige, D.J.; Cooper, W.T.; Glaser, P.H.; Chanton, J.P. Partitioning pathways of $CO_2$ production in peatlands with stable carbon isotopes. *Biogeochemistry* **2013**, *114*, 327-340, doi:10.1007/s10533-012-9813-1.
52. Bond-Lamberty, B.; Bronson, D.; Bladyka, E.; Gower, S.T. A comparison of trenched plot techniques for partitioning soil respiration. *Soil Biol. Biochem.* **2011**, *43*, 2108-2114, doi: 10.1016/j.soilbio.2011.06.011.
53. Larmola, T.; Tuittila, E.S.; Tiirola, M.; Nykanen, H.; Martikainen, P.J.; Yrjala, K.; Tuomivirta, T.; Fritze, H. The role of Sphagnum mosses in the methane cycling of a boreal mire. *Ecology* **2010**, *91*, 2356-2365, doi:10.1890/09-1343.1.
54. Teh, Y.A.; Silver, W.L.; Conrad, M.E.; Borglin, S.E.; Carlson, C.M. Carbon isotope fractionation by methane-oxidizing bacteria in tropical rain forest soils. *J. Geophys. Res.-Biogeosci* **2006**, *111*, doi:10.1029/2005JG000053.
55. Templeton, A.S.; Chu, K.-H.; Alvarez-Cohen, L.; Conrad, M.E. Variable carbon isotope fractionation expressed by aerobic $CH_4$-oxidizing bacteria. *Geochim. Cosmochim.* Acta **2006**, *70*, 1739-1752, doi: 10.1016/j.gca.2005.12.002.

56. Dorodnikov, M.; Marushchak, M.; Biasi, C.; Wilmking, M. Effect of microtopography on isotopic composition of methane in porewater and efflux at a boreal peatland. *Boreal Environ. Res.* **2013**, *18*, 269–279.